Heliyon 9 (2023) e20887

Contents lists available at ScienceDirect

Heliyon

journal homepage: www.cell.com/heliyon

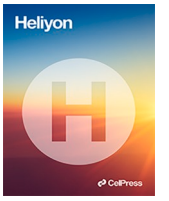

Evaluating screw-shaft pile composite foundations in round Gravelly soil: A study using model tests and numerical simulations

Tingting Yang *, Weicheng Zheng, Yongli Xie, Hongguang Zhang, Xiabing Yue

School of Highway, Chang'an Univ., Xi'an 710064, China

ARTICLE INFO

Keywords:
Screw–shaft pile
Composite foundation
Load transfer
Finite element method

ABSTRACT

Screw-shaft piles have seen extensive adoption in construction and railroad engineering, due to their superior enhanced bearing capacity and cost-effectiveness. While monopiles have been thoroughly examined, composite foundations that include screw-shaft piles have not been studied as extensively. Proper determination of geometric parameters for both the piles and the cushion is a critical aspect of successful design. This paper introduces a comprehensive examination that merges indoor experiments with numerical simulations, aiming to evaluate the bearing capacity, settlement characteristics, and force characteristics of screw-shaft piles under a variety of conditions. This study scrutinizes key components, such as root diameter, pitch, cushion modulus, and the threaded portion's proportion. The research outcomes offer crucial insights for optimizing the design parameters of screw-shaft pile composite foundations. The results indicate that the side resistance of screw-shaft piles initially increases with the threaded section's length, stabilizing at an optimal length of approximately 0.44–0.55 times the pile length (L). Furthermore, although decreasing the pitch improves bearing capacity, it also introduces variations in pile material usage, with optimal bearing performance noted at a pitch approximately equal to the diameter (D). Moreover, screw-shaft piles with thread widths ranging between 0.58D and 0.67D show a significant decrease in stress concentrations, approximately 22 % less than those with a width of 0.5D. By setting the cushion modulus within the 40 MPa–60 MPa range, reduced settlement and optimal pile-soil stress ratios were achieved. These research outcomes provide critical insights into optimizing screw-shaft pile composite foundation design parameters, serving as valuable guidance for designers and engineers in diverse civil engineering projects.

1. Introduction

Pile foundations are widely recognized as one of the most common and essential components in civil engineering [1]. They serve as indispensable solutions for foundations that do not meet design specifications. Over time, diverse engineering demands have driven the emergence of innovative pile forms, such as branch piles [2,3], belled piles [4–6], concrete bored screw piles [7], and screw-shaft piles [8], each distinguished by unique cross-sectional shapes. Among these, piles with threads, such as helical piles [9,10], concrete bored screw piles, and screw-shaft piles, have gained popularity in the industry owing to their advantages of high bearing capacity, material efficiency, and streamlined construction processes. They are extensively used in civil buildings, highways, and railroads [11–14].

* Corresponding author.
E-mail address: ytt965351342@163.com (T. Yang).

https://doi.org/10.1016/j.heliyon.2023.e20887
Received 7 June 2023; Received in revised form 1 October 2023; Accepted 10 October 2023
Available online 11 October 2023

Helical piles, considered a significant advancement in foundation engineering during the latter half of the 19th century [15], exhibit remarkable bearing capacity up to 1.5 times that of conventional grouted piles while conserving approximately 40 % of the concrete usage [16]. However, limitations in helical pile usage arise from equipment constraints and installation depth considerations [17]. Consequently, bored concrete and screw-shaft piles have been introduced as alternatives. Although bored concrete screw piles are effective, they are prone to damage at the top of the pile because of force-related issues [18]. In contrast, screw-shaft piles, a novel pile type, present a promising solution. These piles feature different cross-sections, with a cylindrical head and a threaded bottom [19]. The geometric arrangement of screw-shaft piles distributes additional stresses more efficiently, with smaller stresses at the bottom and larger stresses at the top [20]. Moreover, the variation in the diameter between the upper and lower shafts enhances the resistance and counteracts the larger axial forces at the top [21], resulting in a more balanced distribution of pile stresses. Consequently, screw-shaft piles are widely adopted in engineering projects [22]. Nevertheless, research on the bearing characteristics and design of screw-shaft piles has not kept pace with their practical applications.

Existing research on screw-shaft piles has primarily focused on studying their bearing mechanisms. Several studies that employ different methods [23,24] to examine the bearing characteristics of screw–shaft piles with various soil qualities [8] have been conducted. For instance, Wang et al. [23] performed laboratory model experiments to explore the bearing mechanism of screw-shaft piles and highlighted the significant improvement in lateral resistance and bearing capacity due to the use of threaded design. Similarly, Jiang [24] investigated the bearing capacity of screw-shaft piles in silt and observed a substantial increase in the maximum bearing capacity compared with that of straight piles. Additionally, Chen et al. studied the bearing capacity of screw-shaft piles in sandy soil and observed enhanced load distribution over a larger surface area, leading to a 43 % increase in the maximum load capacity compared to straight piles. The threaded part of the screw-shaft pile can enhance the lateral resistance of the pile and provide vertical support [25–29]. While some studies have identified other influencing factors, such as thread spacing [17,30,31], width [32,33], pile diameter [34], soil quality [27,35,36], and pile installation [37–39], which affect the load-carrying characteristics of piles [17,40], most studies have concentrated on helical piles [41–43] and drilled full-length screw piles [44–47], neglecting overlooking studies on the influencing factors specific to screw-shaft piles. As screw-shaft piles consist of both straight and threaded sections and their bearing characteristics differ from other types of piles [8], it is essential to explore these unique properties rather than solely relying on research related to helical and drilled full-length screw piles.

Furthermore, the behavior of piles in composite foundations differs significantly from that in monopiles owing to the influence of the cushion [24]. Unfortunately, existing research on screw-shaft piles has primarily focused on monopiles [8,21], overlooking the specific bearing characteristics of screw-shaft piles in composite foundations. Given the substantial impact of the geometric parameters on the bearing capacity of composite foundations [48], it is imperative to study the impact of the geometric parameters of screw-shaft piles on the bearing capacity and settlement within composite foundations. Additionally, the choice of the cushion plays a vital role in controlling the stress distribution between the pile and soil, further affecting the bearing capacity of composite foundations [49–51]. Therefore, a thorough examination of the geometric parameters of screw-shaft piles and the cushion is crucial for the rational design of screw-shaft piles.

To bridge these knowledge gaps and achieve the research objectives, this study adopts a combined approach of laboratory experiments and numerical simulations. Load experiments were conducted on both the control and screw-shaft pile composite foundations, with data measured using pressure transducers and strain gauges. Subsequently, a numerical model was developed and validated using experimental results to explore the influence of various geometric parameters of screw-shaft piles, including the thread pitch, length of the thread section, root diameter, and cushion modulus, on the bearing capacity and settlement behavior of composite foundations. This study aims to identify the appropriate design parameters for screw-shaft piles, providing valuable insights for their selection and effective implementation in composite foundations.

In conclusion, this study aims to enhance the understanding of the bearing characteristics and design considerations for screw-shaft piles, facilitating their optimal utilization in various civil engineering projects. The findings of this study serve as a basis for optimizing the design of screw-shaft pile composite foundations, with the ultimate goal of promoting their wider application in housing construction engineering, railroad engineering, and foundation treatment.

2. Model test

For indoor tests, the civil engineering methodology is to use a downscaled model to enhance cost-effectiveness and efficiency while maintaining a reasonable representation of real-world conditions [52]. For our case, the geometric similarity ratio between the prototype and model was selected to be 10, as guided by the site conditions and mechanical indices of the model material, as listed in Table 1.

The original gravel soil from Hanzhong, Shaanxi Province, China, was reduced by a factor of 10 to mitigate the particle size effect [53]. River sand was selected as a suitable replacement owing to its appropriate mechanical properties and particle sizes. The detailed physical properties of the test soils are listed in Table 2. Approximately 0.7 m^3 of river sand was filled into the container, creating a

Table 1
Similarity ratios for laboratory model tests.

Physical parameters	Geometric dimensions	Surface area	Modulus	Pressure
Similarity Relation	C_l	C_A	C_E	C_F
Similar Constant	10	100	8.18	818

final soil layer height of approximately 1 m. To ensure proper soil density, the soil was compacted in layers, with each layer being 10 cm thick. Adequate compaction is crucial for achieving uniform soil distribution.

To simulate the compressive performance of screw-shaft piles, the model pile material needs to satisfy both the similarity ratio requirements and match the actual mechanical properties of typical engineering materials. Grouted piles commonly used in engineering have an elastic modulus ranging from 28 to 31.5 GPa [54]. Considering the similarity ratio, the model pile required an elastic modulus ranging from 3.42 to 3.85 GPa. The average elastic modulus of uniaxial compression tests of epoxy glass rods was found to be 3.47 GPa, and the screw thread of the pile body was easily processed using a lathe. Therefore, the model pile was constructed using epoxy glass rods with an elastic modulus E = 3.47 GPa. Table 3 lists the geometric specifications and material properties of the model piles, where the screw-shaft pile has a length of 700 mm and a diameter of 60 mm. To monitor the force of the pile, strain gauges were affixed to the pile body in advance, and the strain gauges, with a resistance value of 120 and spaced 100 mm apart, were symmetrically arranged on both sides of the pile.

To ensure uniform loading, a cushion with a radius of 125 mm was employed; its material properties are listed in Table 2. A 2 cm-thick iron plate was used as the loading plate to prevent excessive deformation of the loading plate during loading. Holding load test was selected as the loading method, with load values during each stage ranging between 1/8 and 1/10 of the predicted bearing capacity, conforming to the code and reference guidelines [55].

Considering the boundary effects [56], the selected model test configuration is illustrated in Fig. 1. To minimize boundary effects, petroleum jelly was applied to all four sides of the container. The container was placed on a solid surface with dimensions of 0.8 m (L) × 0.8 m (W) × 1.2 m (D). The container was constructed using square welded steel without a top lid. To ensure rigidity, 20 mm thick clear tempered glass panels were fitted on all four sides [8]. Adequate space inside the box was available to accommodate the soil and piles. The pile was covered with a 2 cm-thick layer of cushioning material, followed by a 2 cm thick circular loading plate. The loading plate featured a JLBU-1 load cell at the center and a WBD displacement sensor on the side. A hydraulic jack was connected to the reaction frame above the load cell, allowing the application of a downward force on the load plate. Strain data were acquired using a TDS-530 data collector, which has the functionality of storing the data on a memory card so that it can be retrieved at any time. The experimental procedure is illustrated in Fig. 1.

The study included two test groups: a screw-shaft pile composite foundation group and control pile composite foundation group. Settlement data collected using WBD displacement transducers was used to construct the load-settlement curve, also known as the P–S curve. The strain gauges provided strain values, which were then converted into pile stress values using Equation (1). These stress values were used to determine the pile axial force and lateral pile friction. Subsequently, the corresponding curves were plotted, and a comparative analysis was conducted between the experimental outcomes of the two groups to investigate the differences in bearing characteristics and settlement behavior.

$$\sigma_i = E \times \varepsilon_i \tag{1}$$

where σ_i is the stress within the pile body (kPa); E is the elastic modulus of the pile body material, which is an epoxy glass wire rod used in this experiment, with a value of $E = 3.47$ GPa; and ε_i is the strain of the pile body.

3. Results and discussion

3.1. Load-settlement curves

The load-settlement (P–S) lines of both screw-shaft and straight pile composite foundations are illustrated in Fig. 2. These serve as crucial indicators of the bearing capacity of the composite foundation [57]. In the figure, P represents the load F to load area A ratio, and S indicates the settlement value obtained from the WBD displacement transducers. It can be observed that during the initial loading stages, both foundations exhibit similar P–S curves, suggesting a linear relationship and the potential presence of an elastic region between the pile and ground, where the shape of the pile had not yet begun to play a role. The similarity in the P–S curves implies that the threaded section of the screw-shaft pile has a negligible effect on the load-bearing capacity, particularly under small loads. In this arrangement, the friction between the pile and foundation ground plays a dominant role in the load-bearing ability [28].

As the load increases, the slopes of the curves also increase. Notably, the P–S curve of the screw-shaft pile composite foundation is higher than that of the straight pile composite foundation (as shown in Fig. 2), indicating a higher bearing capacity for the former, which is in accordance with results of previous studies [14]. This phenomenon can be attributed to the presence of the threaded portion, which transfers the applied force to the adjacent soil, thereby sharing the load and enhancing the bearing capacity [27].

According to the Technical Code for Ground Treatment of Buildings, the stress corresponding to a 0.12D settlement is chosen as the characteristic value of the bearing capacity of the composite foundation [55]. Based on this guideline, the screw-shaft pile composite

Table 2
Material parameters of the foundation soil in the model.

Materials		E (MPa)	γ (KN/m^3)	ω (%)	C (kPa)	φ (°)
River sand	Prototype	73.5	20	3.42	4.74	30.05
	Model	8.99	17.94	3.42	0.58	30.05
Cushion	Prototype Model	20	22	3	3	30
		2.4	19.73	3	0.37	30

Table 3
Material parameters of the model pile.

Materials		Pile length(m)	Pile diameter(m)	Cross-sectional area(m^2)	Elastic modulus(MPa)	Compressive strength(MPa·m^2)
Pile	Prototype	7	0.6	0.283	2.84×10^4	5566
	Model	0.7	0.06	2.83×10^{-3}	3.47×10^3	6.80

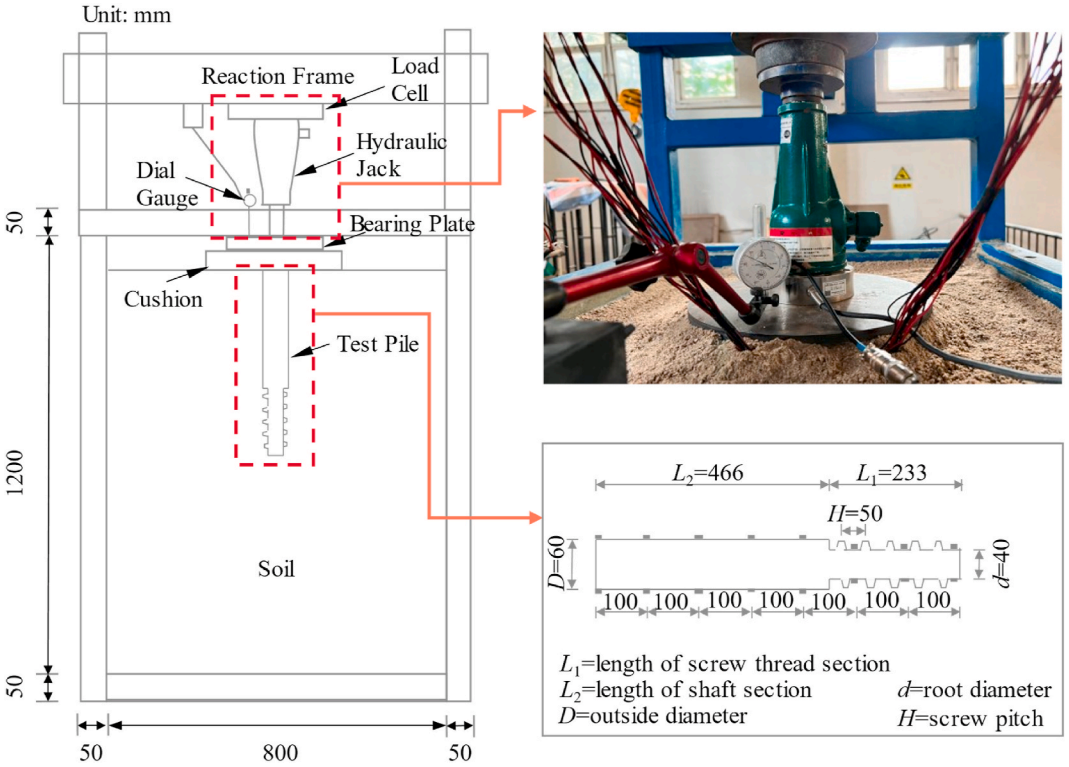

Fig. 1. The procedure for the experiment.

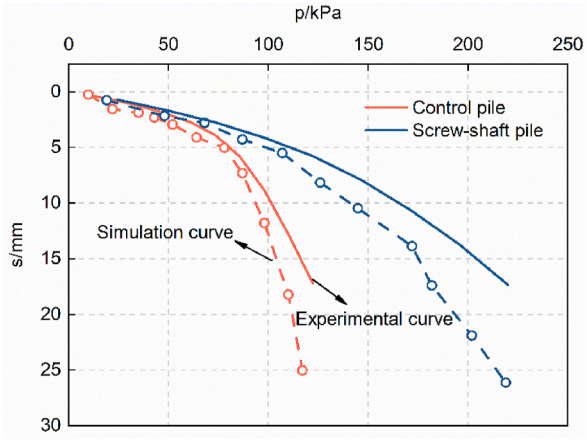

Fig. 2. The load-settlement curve.

foundation exhibited a bearing capacity characteristic value of 71 kPa, whereas the straight pile composite foundation exhibited a value of 39 kPa. The screw-shaft pile composite foundation exhibited an 82.1 % increase in the characteristic load-carrying capacity and a 16.92 % reduction in material usage compared to the straight pile composite foundation. These results clearly demonstrate the

significant advantages of the screw-shaft pile composite foundations for foundation design.

3.2. Pile bearing characteristics

The load-carrying capacity of a composite foundation is significantly influenced by the pile characteristics, which encompass both the side and end resistances. The observed differences in the side and end resistances highlight the distinct load-bearing behaviors of screw-shaft and straight piles when subjected to similar conditions [17]. In this study, strain gauges were utilized to measure the strain on the pile, enabling an estimation of the axial force and side resistance based on these measurements. The results are shown in Fig. 3.

Fig. 3 shows the axial force and side resistance of both the screw-shaft piles and straight piles in the composite foundations under a load corresponding to the ultimate bearing capacity of the straight pile composite foundation. Notably, clear trends can be observed in the axial force for both the screw-shaft and straight piles. In the screw-shaft pile, the axial force gradually increases and then decreases from top to bottom, whereas in the straight pile, it consistently decreases, as supported by the findings in previous studies [19]. Interestingly, the axial force of the screw-shaft pile was significantly lower than that of the straight pile within the height ranging between 50 cm–80 cm, which coincides with the threaded portion of the screw-shaft pile. The side resistance at this height for the screw-shaft pile, calculated using Equation (2), is approximately 7 times greater than the corresponding section in the straight pile, with values of 14.45 kPa and 2.18 kPa, respectively. Under the same load, the average side resistance of the straight pile was approximately 3.31 kPa, whereas the screw-shaft pile exhibited a remarkable improvement of 143.2 % with a value of approximately 8.05 kPa over the straight pile. However, a closer comparison reveals that the side resistance of the screw-shaft pile is smaller than that of its threaded section, indicating that the increase in side resistance mainly relies on the threaded section. This can be attributed to the presence of threads resulting from differences between the inner and outer pile diameters. The action of the load causes the threads of the helical section and foundation to interact with each other, enhancing the interaction and thus increasing the side resistance of the threaded section of the screw-shaft pile, which is a phenomenon reported in the previous studies [32]. Nonetheless, we also observed a unique finding wherein the screw-shaft pile exhibited negative side resistance near its top. This was attributed to the presence of a straight rod section that penetrated the cushion layer under the applied load, leading to an upward movement of the pile with respect to the surrounding soil.

$$q_{si} = (Q_i - Q_{i-1}) / (L_i \pi D) \tag{2}$$

where, q_{si} is the average value of pile side resistance in the section "i" of the pile body (kPa), L_i is the length of the unit in the section "i" of the pile body (m), and D is the outer diameter of the pile (m).

Additionally, Fig. 3 indicates that the end resistance of the straight pile is three times greater than that of the screw-shaft pile, with values of 0.95 kN and 0.33 kN, respectively. This reduction in end resistance can be attributed to the increased side resistance, which redistributes the load borne by the pile, resulting in a reduced end resistance.

Based on the observed axial force and end-resistance curves of the piles, we conclude that the screw-shaft pile composite foundation exhibits superior load-carrying capacity compared to the straight pile composite foundation. Specifically, at a given load level, the side resistance of the screw-shaft pile accounted for 73 % of the total load carried by the pile, whereas the end resistance accounted for 27 %. In contrast, the side resistance of the straight pile accounted for 28 % of the load, and the end resistance accounted for 72 %. Moreover, the average side resistance of the screw-shaft piles was nearly 2.5 times that of the straight piles, whereas the end resistance was approximately one-third that of in the straight piles. This suggests that the bearing capacity of the soil under the screw-shaft pile was not fully utilized, indicating the potential of the screw-shaft piles to withstand even higher loads. The primary improvement in the bearing capacity of the screw-shaft pile is attributed to the enhanced side resistance, achieved through the action of the screw threads, which outperforms the side resistance of the straight pile. The soil body at the bottom of the pile remains unchanged; thus, its

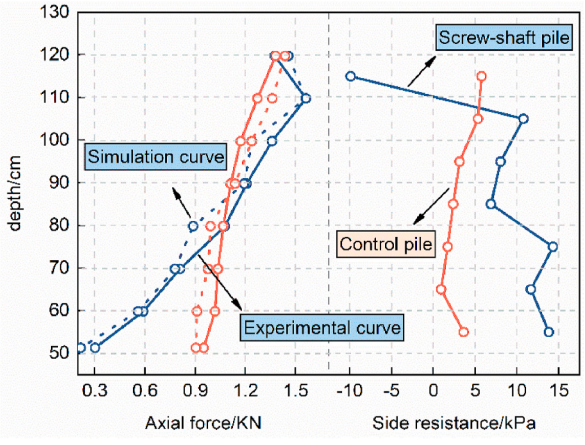

Fig. 3. The axial forces and frictional resistance of the pile.

maximum end resistance remains constant. However, the improvement in side resistance, resulting from the screw threads enhances the bearing capacity of the pile body. Therefore, the improvement in the bearing capacity of the screw-shaft pile is mainly attributed to its enhanced side resistance.

4. Simulation

4.1. Numerical method

Exclusively relying on indoor tests for research is time-consuming and labor-intensive, often leading to challenges in data acquisition and limited repeatability. Moreover, some data might not be available. Numerical simulation methods are valuable in addressing these limitations. These methods offer easy data acquisition and enable multiple simulation repetitions, as demonstrated in several studies [17,34,35,39,51]. Therefore, this study, a combined approach that incorporates both indoor tests and numerical simulations was adopted to overcome these limitations. To analyze the effects of pile geometry and cushion parameters on the bearing capacity and settlement of composite foundations, a Fast Lagrangian Continuum Analysis (3D) was employed. The numerical model depicted in Fig. 4 was utilized with a computational domain centered at the bottom of the foundation spanning an 8 m × 8 m area in the x-y plane. The computational depth in the z-direction extended to 12 m below the bottom of the cushion, and the size of the computational area was established based on the geometrical similarity. Specifically, the dimensions of the original indoor test model were scaled by a factor of 10 to establish the size of the computational area.

To maintain consistency, the model pile was scaled up by 10 times compared to the pile geometry depicted in Fig. 1. The material parameters for the numerical simulation were determined based on the values listed in Table 4. Preprocessing external software was used to generate the model and mesh, which were subsequently imported into the numerical analysis software. The mesh around the piles was refined to enhance the computational accuracy.

The foundation's vertical face was constrained by the horizontal displacement, whereas the bottom of the model was constrained by the vertical displacement, as described previously [17]. For computational simplification, homogeneity and isotropy were assumed for the loading plate, pile, soil, and cushion layers. The ground and cushion layers were modeled as ideal elastic-plastic materials, whereas the piles and loading plate exhibited linear elasticity [39]. To account for the significant differences in material properties and stiffness, contact surface units were established between different materials using the move-out and move-in methods.

The contact surface cells were created using the move-out and move-in methods, with the corresponding parameters determined using Equation (3), which governs the interactions among the materials.

$$k_n = k_s = 10 \times \max((K + 4/3 \times G)/\Delta z_{\min}) \tag{3}$$

where k_n is the normal spring stiffness in the contact surface cell, k_s denotes the tangential spring stiffness in the contact surface cell, K denotes the bulk modulus, G denotes the shear modulus, and $\Delta z_{\min}$ denotes the minimum normal scale on both sides of the contact surface grid.

The data were collected using the Fish function, a programming statement in the software, to derive the pile stress, soil stress, and settlement values of the loading plate. The loading method employed in the simulation mirrored the model test and used a load maintenance method.

To validate the accuracy of the bearing capacity and settlement in the numerical simulations, a screw-shaft pile and straight pile

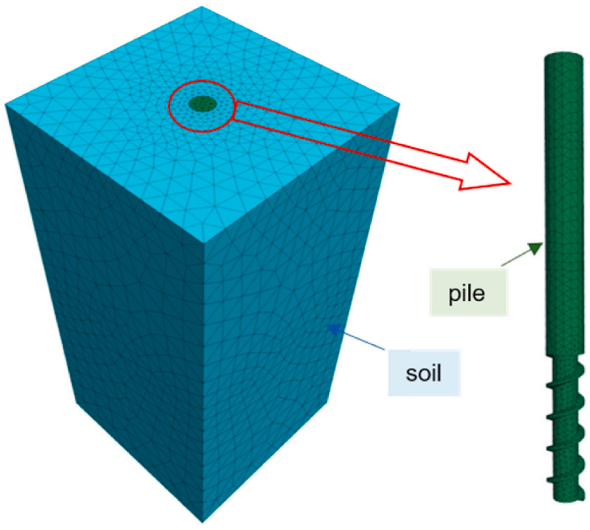

Fig. 4. Numerical model.

Table 4
Parameters of the numerical model for composite foundations.

Material	ρ (kg/m^3)	E (MPa)	K (MPa)	G (MPa)	C (kPa)	φ (°)
Plate	2500	2.06×10^5	1.14×10^5	8.58×10^4	/	/
cushion	2200	20	13.3	8	3	35
pile	2500	2.84×10^4	1.58×10^4	1.18×10^4	/	/
soil	1980	73.5	72.06	27.63	0	30.05

were used, both scaled 10 times in dimensions compared with the indoor tests. The material parameters of these piles are listed in Table 4. The results obtained from the numerical simulations were scaled down according to the similarity scale in Table 1 before being compared with the laboratory model test results.

Figs. 2 and 3 show a comparison of the settlement and axial force curves from the two sets of results, demonstrating a good fit between the numerical simulation and indoor test curves. As corroborated by Meng et al. [17], the matching load settlement curves and axial force curves confirm the effectiveness of numerical modeling in studying the pile bearing capacity and settlement. Thus, we employed this model to further investigate the effects of the pile and cushion parameters on the bearing characteristics and settlement control of composite foundations.

4.2. The proportion of screw section

The interlocking effect between the threads of screw-shaft piles and the surrounding soil has been shown to significantly enhance the bearing capacity when compared to conventional straight pile composite foundations, as discussed in Section 3.2. Consequently, it is essential to investigate the influence of the proportion of the threaded portion, as it directly affects the bearing performance of the composite foundation. In this study, the numerical model discussed in Section 4.1 was employed to simulate screw-shaft piles with varying proportions of threaded sections, specifically 33 %, 44 %, 55 %, and 66 %. The objective was to explore the effect of the threaded portion proportion on the bearing capacity and settlement of the composite foundation.

(1). Load-settlement analysis

Fig. 5 illustrates the load-settlement curves of composite foundations with screw-shaft piles featuring different proportions of threaded sections. The ultimate bearing capacities of the composite foundation, as observed in the figure, are 1254, 1284, 1308, and 1328 kPa, respectively. Notably, these values are significantly higher than the 700 kPa bearing capacity of the straight pile, exhibiting increases of 79.14 %, 83.43 %, 86.86 %, and 89.71 %, respectively. This progressive increase in the bearing capacity of the screw-shaft pile composite foundation can be attributed to the enhanced side resistance provided by the threaded segments, as discussed in Section 3.2. Consequently, screw-shaft piles with longer threaded segments offer greater side resistance, resulting in higher bearing capacities.

The effect of the proportion of the threaded portion on the load-settlement relationship was assessed by statistically analyzing the settlement differences at various load levels. A clear trend emerged from the graphs, revealing that changes in the proportions of the threaded sections have a more pronounced impact on the settlement of the composite foundations at higher loads. For instance, at an applied load of 400 kPa, increasing the proportion of threaded sections from 33 % to 66 % led to settlement decreases of 4.86 %, from 16.65 mm to 15.84 mm. However, when the load increased to 1200 kPa, the settlement reduced from 79.08 mm to 62 mm, representing a significant decrease of 21.6 %. This difference in settlement behavior is because at lower loads, as observed in the P–S curve, the load of 400 kPa is still in the elastic stage, resulting in relatively small settlements, where the interaction between the threads and sand is not fully activated, and variations in the pile surface (or screw cross-section) have a minimal impact on the settlement.

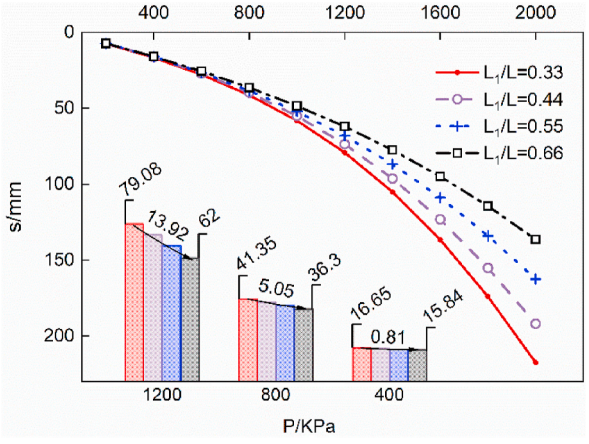

Fig. 5. Load-settlement relationships with different proportions of threaded sections.

However, as the load increased, the threaded section became more influential, leading to distinct settlement differences between the composite foundations with varying proportions of threaded segments.

The distribution of the displacement field can provide valuable insights into the deformation distribution pattern and bearing mechanism of a composite foundation with screw-shaft piles, as also observed in the related literature [21]. Fig. 6 illustrates the displacement field distribution around the pile under a 1200 kPa load for various thread section ratios. A comparison between Fig. 6(a) and (b) reveals that, compared with the straight pile composite foundation, the screw-shaft pile composite foundation exhibits displacement generation in the soil around the threaded section. This was due to the occlusal effect created by the threaded section interacting with the surrounding soil, causing settlement both in the soil around the screw-shaft pile and in the pile itself under the applied load. Consequently, the soil around the screw-shaft pile experienced larger settlement than that around the straight pile. However, the distribution of the soil displacement field around the bottom threads weakened when the proportion of the threaded portion increased from 55 % to 66 %. This observation suggests a reduction in the interlocking effect between the bottom threads and surrounding soil, indicating that the bottom threads may not be fully functional in providing additional bearing capacity.

(2). Stress analysis of piles

Fig. 7 illustrates the distribution of the percentages of side and end resistances and the stress ratio (the ratio of stress at the top of the pile to the stress in the soil around the pile). Zhao et al. [58] emphasized that the pile-soil stress ratio is a crucial parameter in designing a composite foundation and serves as a significant index reflecting the operational characteristics of the composite foundation and load-bearing deformation calculation. This study considered piles with varying thread-section ratios. As depicted in the figure, the stress ratio between the pile and soil decreases with an increase in the ratio of the threaded sections. This phenomenon can be attributed to the interlocking effect of the threaded sections resulting from a higher thread-section ratio, which increases the interlocking effect between the pile and soil. Consequently, a larger area of the ground around the pile begins to bear the load, which causes a decrease in the load carried by the pile, and consequently reduces the pile-soil stress ratio.

Based on the aforementioned analysis, it can be deduced that a smaller pile-to-soil stress ratio is preferable when the foundation soil exhibits good properties. This choice maximizes the utilization of the foundation's bearing capacity, thereby reducing the overall costs.

Furthermore, the observations reveal that Q_p/Q tends to decrease, whereas Q_s/Q tends to increase with an increase in the ratio of threaded segments. The slope of the curve decreases with an increase in the ratio of threaded segments, indicating that a continuous increase in the proportion of threaded segments did not result in a constant increase in Q_s/Q. This phenomenon can be explained by referring to Fig. 6, where the interlocking effect of the pile-bottom threads in Fig. 6(d) and (e) is weaker than those in Fig. 6(b) and (c). Consequently, the threads at the bottom of the pile in Fig. 6(d) and (e) are not fully functional, affecting the exertion of side resistance and leading to a decreased load carried by the pile compared to the case when the threads are fully functional. Consequently, the increase in the load carried by the pile increases gradually, leading to a gradual flattening of the curve and a reduction in the slope.

Fig. 8(a)–8(d) illustrate the distribution of pile stresses for varying screw section ratios. In Fig. 8, the stress diagram of the screw-

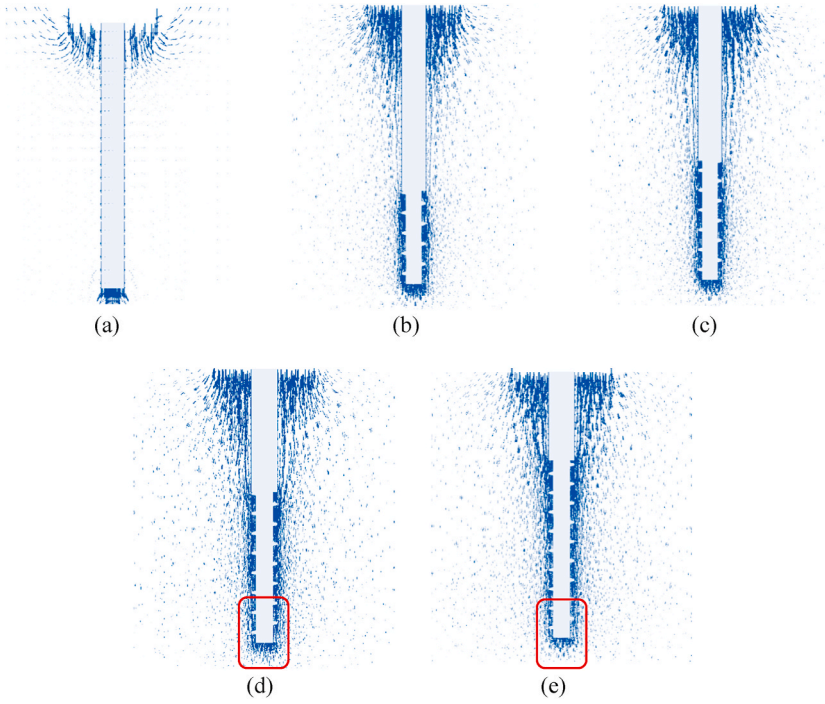

Fig. 6. The distribution of the displacement field of the soil around the pile (a: Composite foundations with straight piles, b: 33 %, c: 44 %, d: 55 %, e: 66 %).

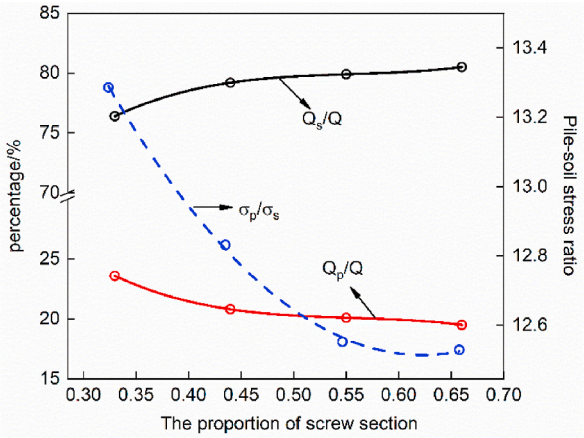

Fig. 7. Distribution of side resistance, end resistance to load ratio and pile to soil stress ratio.
Note: Q_p is the end resistance, Q_s is the side resistance, and Q is the load; σ_p is the stress applied on the pile, σ_s is the stress applied on the soil surrounding the pile; σ_p/σ_s is the pile-soil stress ratio, which represents the stress distribution between the pile and the soil.

shaft pile body demonstrates that stress concentration tends to occur in the first diameter change section of the pile body. Moreover, the stress concentration increased with an increase in the proportion of threaded sections. This phenomenon can be attributed to the decrease in the cross-sectional area of the connection between the straight and threaded sections. The reduction in area leads to a decrease in the compression stiffness according to the compression stiffness (*EA*) equation, resulting in stress concentration in this region. The relationship between the proportion of the threaded section and the stress concentration can be explained by the decrease in the length of the straight section as the proportion of the threaded section increases. The length of the straight section decreases for screw–shaft piles with longer threaded sections. As noted by Zhang et al. [59], the load transfer occurred gradually from the top of the pile downward. Therefore, a shorter straight section produces a smaller friction force and bears a smaller load than a long straight section. Consequently, the load borne by the long threaded section is larger, leading to an increase in the stress concentration.

The analysis indicated that utilizing a threaded section ratio of 44 %–55 % optimized the side resistance of the pile and efficiently utilized the surrounding land. The stress concentration in the variable section was not significant, and the pile-soil stress ratio remained moderate. These conditions improved the bearing capacity of the composite foundation to some extent and reduced the settlement. Therefore, after conducting a comprehensive comparative study, it was concluded that a screw section ratio of 44%–55 % was optimal.

4.3. Thread pitch

The study conducted by Ma et al. [32] highlighted the crucial role of screw-shaft pitch sparseness in determining the helical blade spacing and angle, directly impacting the load-bearing characteristics of screw-shaft piles and making pitch a significant parameter in the design process. For this study, a standard model pile with a thread pitch of 500 mm (H/D = 0.83) was selected, and models were

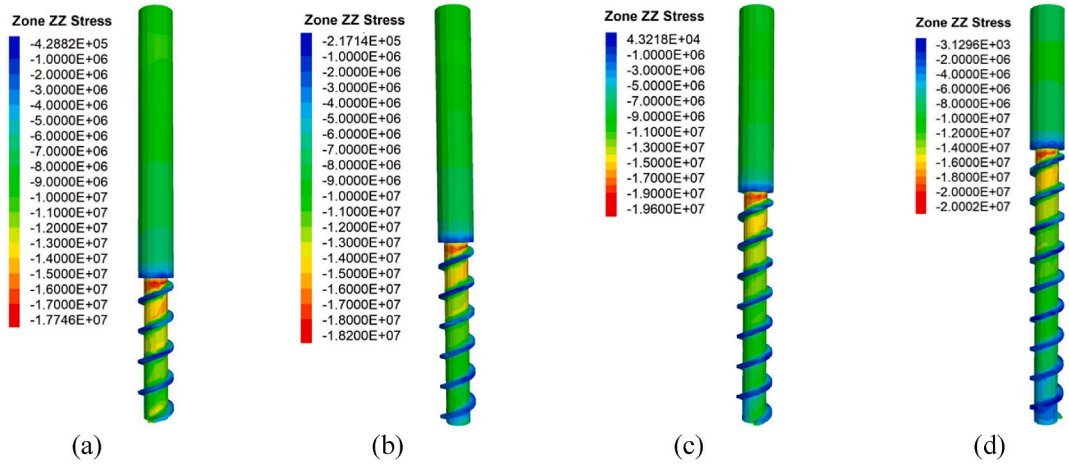

Fig. 8. Stress nephogram of the pile (a: $L_1/L = 0.33$, b: $L_1/L = 0.44$, c: $L_1/L = 0.55$, d: $L_1/L = 0.66$).

developed to explore the impact of the pitch on the pile behavior. Three different thread pitches were considered: 300 (H/D = 0.5), 500 (H/D = 0.83), 700 (H/D = 1.17), and 900 (H/D = 1.5) mm.

(1) load-settlement analysis

Fig. 9 presents the load-settlement curves of the composite foundations constructed with screw-shaft piles with varying thread pitches. The load-carrying capacities of the screw-shaft pile composite foundations were 1269, 1254, 1232, and 1213 kPa at 300 mm (H/D = 0.5), 500 mm (H/D = 0.83), 700 mm (H/D = 1.17), and 900 mm (H/D = 1.5), respectively. Notably, reducing the thread pitch from 900 mm (H/D = 1.5) to 300 mm (H/D = 0.5) resulted in a 4.62 % increase in the load-carrying capacity. This indicates that a decrease in the thread pitch had a minimal impact on the load-carrying capacity of the composite foundations.

The settlement of the composite foundation was examined at various loading levels. The results indicate that the load has a minor effect on the settlement difference of screw-shaft pile composite foundations with varying thread spacings. For instance, at a load of 400 kPa, reducing the thread spacing from 900 mm (H/D = 1.5) to 300 mm (H/D = 0.5) decreased the settlement from 17.21 mm to 16.47 mm, corresponding to a reduction of 4.3 %. At 1200 kPa, the settlement decreased from 89.44 mm to 75.88 mm, equivalent to a reduction of 15.16 %. The difference in settlement at 1200 kPa was only 10.86 % compared to that at 400 kPa, which was less than the value of 16.74 % attributed to the change in the length of the threaded section. Based on this analysis, it can be concluded that a decrease in the thread pitch has a slight impact on the settlement of the composite foundations.

To assess the economic efficiency of screw-shaft piles with different pitches, the utilization rate of the pile material, which is the load-bearing capacity per unit volume of material, was as a reference indicator. The pile material utilization rates for the four screw-shaft piles were 4095 kN/m^3, 4068 kN/m^3, 4040 kN/m^3 and 3987 kN/m^3.

Fig. 10 illustrates the utilization of the pile material in composite foundations constructed with screw-shaft piles with varying thread pitches. The graph indicates that as the pitch decreases, the pile material utilization tends to increase initially and then decreases. The optimal load-carrying capacity is observed at a pitch of approximately 500 mm (H/D = 0.83).

(2). Stress nephogram of pile

Fig. 11 illustrates the stress nephrogram of screw-shaft piles with varying proportions of threaded sections under a load of 1200 kPa. The plot depicts the distribution of the side and end resistances, along with the pile-soil stress ratios. It is evident that decreasing the thread pitch resulted in a reduction in the pile-soil stress ratio. This outcome can be attributed to the improved interlocking effect between the pile and the surrounding soil as the thread pitch decreased. As a result, a larger portion of the soil surrounding the pile bears the load, leading to a decrease in the load carried by the pile and, consequently, reducing the stress ratio between the pile and soil.

Moreover, as the thread pitch decreased, Q_p/Q decreased steadily, whereas Q_s/Q increased progressively. However, the rate of increase in Q_s/Q gradually decreased. This indicates that reducing the thread pitch only enhances the side resistance up to a certain point. Beyond this point, excessively narrow thread pitches offer limited effectiveness in improving the side resistance, leading to inefficient utilization of the pile material.

Fig. 12 (a)–Fig. 12 (d) illustrate the distribution of pile stresses for varying thread pitches. Analysis of the stress nephrogram (Fig. 12) further revealed that stress concentrations mainly occurred in the first variable section of the pile. With an increase in the thread pitch, the stress concentration decreases, whereas the stress concentration zone gradually expands. This behavior can be attributed to the correlation between the stress concentration and pile cross-section variation. Specifically, as the thread spacing increased, the first variable cross-sectional area expanded, leading to a larger area of influence and, subsequently, an expanded stress concentration area. Moreover, a larger first variable cross-sectional area exhibited a higher side resistance owing to the pile-soil interactions. This interaction reduces the force on the first variable cross-section, resulting in a lower stress concentration.

Considering the aforementioned factors, a thread pitch of approximately 1D is deemed preferable because it strikes a balance

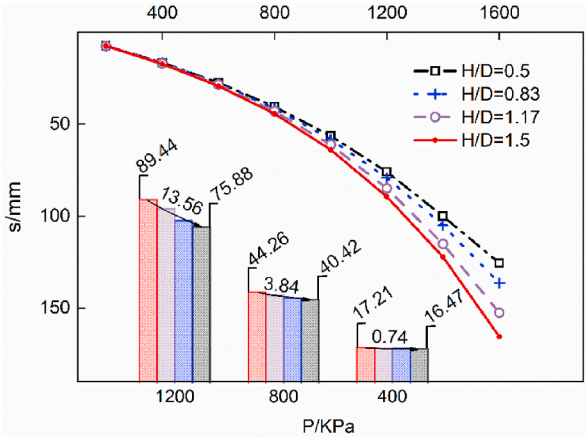

Fig. 9. Load-settlement relationships with different thread pitches.

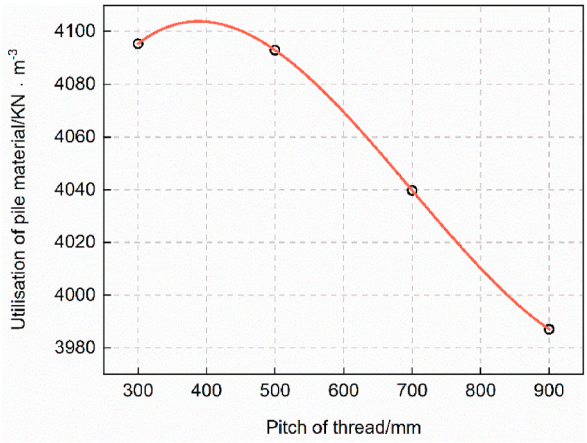

Fig. 10. The utilization of pile material for composite foundations with different thread pitches.

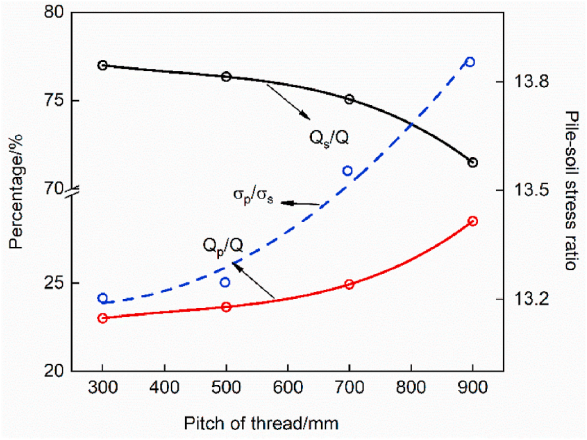

Fig. 11. Distribution pattern of pile side resistance and end resistance.

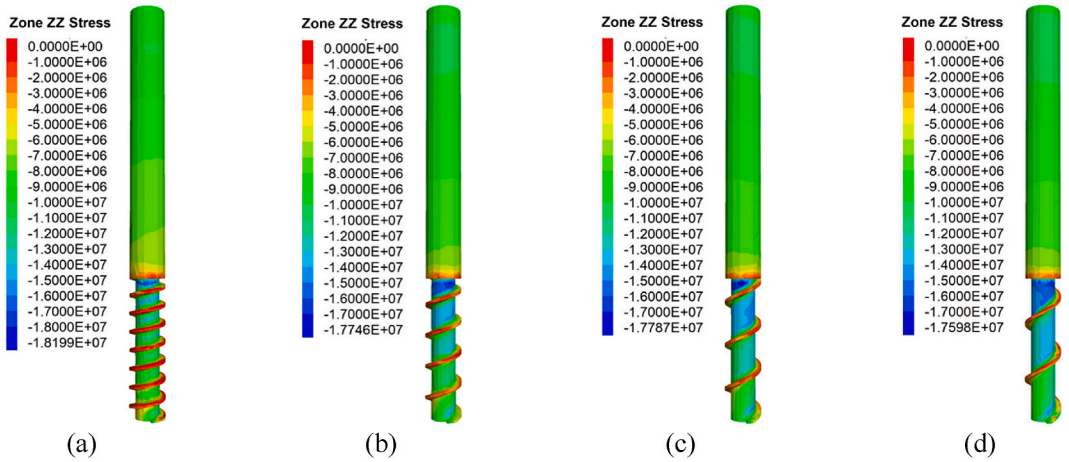

Fig. 12. Stress nephogram of the pile (a: H/D = 0.5, b: H/D = 0.83, c: H/D = 1.17, d: H/D = 1.5).

between minimizing the stress concentration values and maintaining an optimal stress concentration zone.

4.4. Root diameter

Screw-shaft piles demonstrate a higher load-carrying capacity than straight piles owing to their threaded design, which improves the mechanical interaction between the pile and soil. Understanding the root diameter of screw-shaft piles is crucial, as it directly influences the contact area between the pile and soil, ultimately affecting the load-carrying capability of the piles. In this study, a composite foundation of screw-shaft piles with a root diameter of 400 mm (d/D = 0.67) was used as the standard model. To explore the impact of the root diameter, numerical models were developed for screw-shaft pile composite foundations with root diameters of 300 mm (d/D = 0.5), 350 mm (d/D = 0.58), 400 mm (d/D = 0.67), and 450 mm (d/D = 0.75).

(1) load-settlement analysis

Fig. 13 displays the load-settlement curves of the composite foundations of screw-shaft piles with varying root diameters. The bearing capacities of the composite foundations with root diameters of 300 (d/D = 0.5), 350 (d/D = 0.58), 400 (d/D = 0.67), and 450 mm (d/D = 0.75) were 1290, 1272, 1254, and 1243 kPa, respectively. Notably, reducing the root diameter from 450 mm (d/D = 0.75) to 300 mm (d/D = 0.5) resulted in a marginal 3.64 % increase in the bearing capacity of the composite foundations. This suggests that the reduction in root diameter had a limited impact on load-bearing capacity.

Furthermore, Fig. 13 illustrates the effect of the root diameter on the settlement of the composite foundations. The figure indicates that the load had a minor effect on the settlement differences of the composite foundations with screw-shaft piles with different root diameters. Under a load of 400 kPa, reducing the root diameter from 450 mm (d/D = 0.75) to 300 mm (d/D = 0.5) resulted in a settlement reduction from 16.72 mm to 16.33 mm, a decrease of 2.33 %. Similarly, under loads of 800 kPa and 1200 kPa, the settlement decreased from 42.21 mm to 39.36 mm (a reduction of 6.75 %) and from 82.1 mm to 72.38 mm (a reduction of 11.84 %), respectively. These findings suggest that the root diameter has limited influence on the settlement reduction in composite foundations.

Fig. 14(a)–14(d) shows the displacement field distribution of the soil surrounding the pile under a load of 1200 kPa under four different conditions. The diagram reveals that during the loading of the composite foundation, the soil adjacent to the pile underwent a downward displacement along with the threads of the pile. Interestingly, an increase in the root diameter leads to a reduction in the affected area where the threads engage with the soil while simultaneously expanding the region where settlement occurs at the end of the pile. This phenomenon can be attributed to the diminishing width of the threads as the root diameter increases, resulting in a weaker mechanical interlock between the threads and surrounding soil. As a result, the interaction between the threads and soil becomes narrower, leading to a decrease in the extent of mechanical interlocking with increasing root diameter.

(2). Stress analysis of pile

Fig. 15 presents the profiles of the side resistance, end resistance, and pile-to-soil stress ratio for screw-shaft piles under a load of 1200 kPa with varying root diameters. Remarkably, a decrease in root diameter resulted in a reduction in the stress ratio between the piles and surrounding soil. This was because of the wider thread profile associated with smaller root diameters, which enhanced the interlocking mechanism between the piles and soil. Consequently, a larger proportion of the load is carried by the soil, leading to an increase in the soil load and a decrease in the pile load, ultimately resulting in a decreased pile-to-soil stress ratio.

Furthermore, as the root diameter decreased, Q_p/Q gradually decreased, whereas Q_s/Q steadily increased. However, the rate of increase in Q_s/Q progressively decreased with decreasing root diameter, indicating that the enhancement of side resistance through root diameter reduction has limitations. Small root diameters exhibited minimal improvements in side resistance and offered little significance in enhancing overall performance.

Fig. 16(a)–16(d) depicts the stress distribution patterns in screw-shaft piles with varying root diameters. The figure clearly indicates

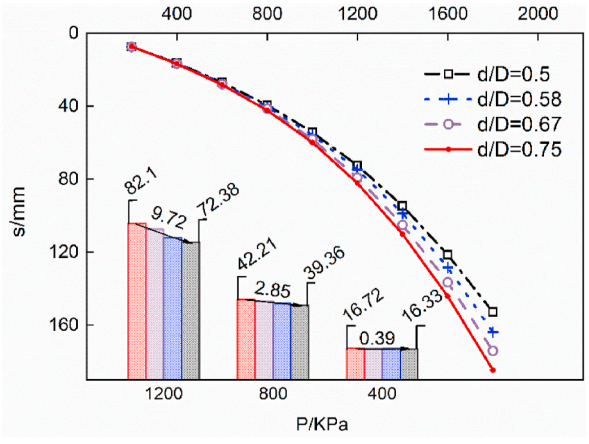

Fig. 13. Load-settlement relationships with different root diameters.

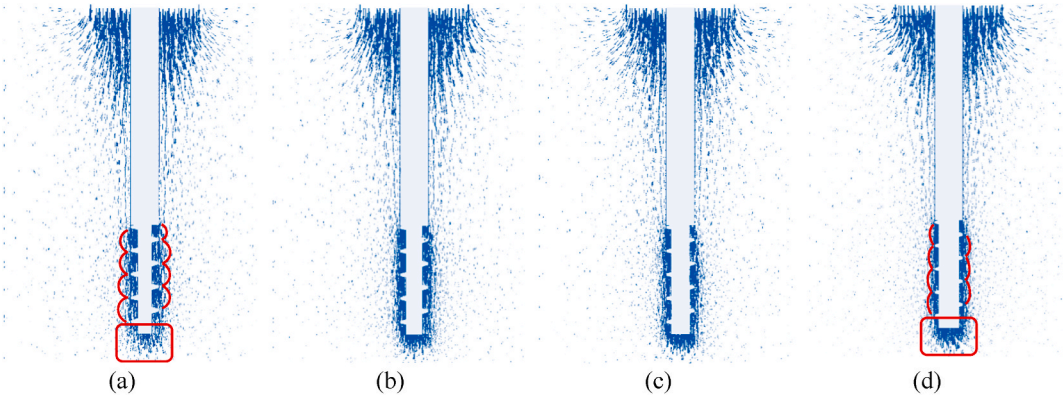

Fig. 14. The distribution of the displacement field of the soil around the pile (a: d/D = 0.5, b: d/D = 0.58, c: d/D = 0.67, d: d/D = 0.75).

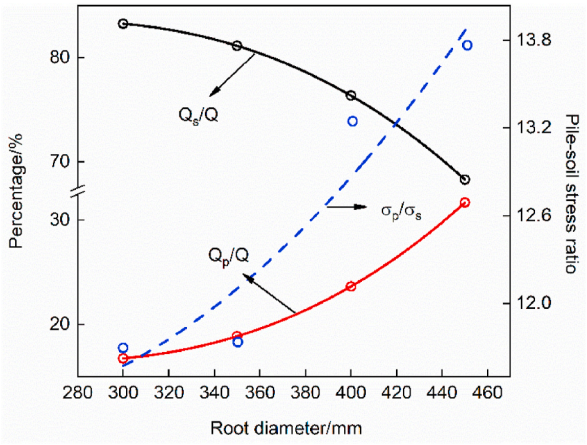

Fig. 15. Distribution pattern of pile side resistance and end resistance.

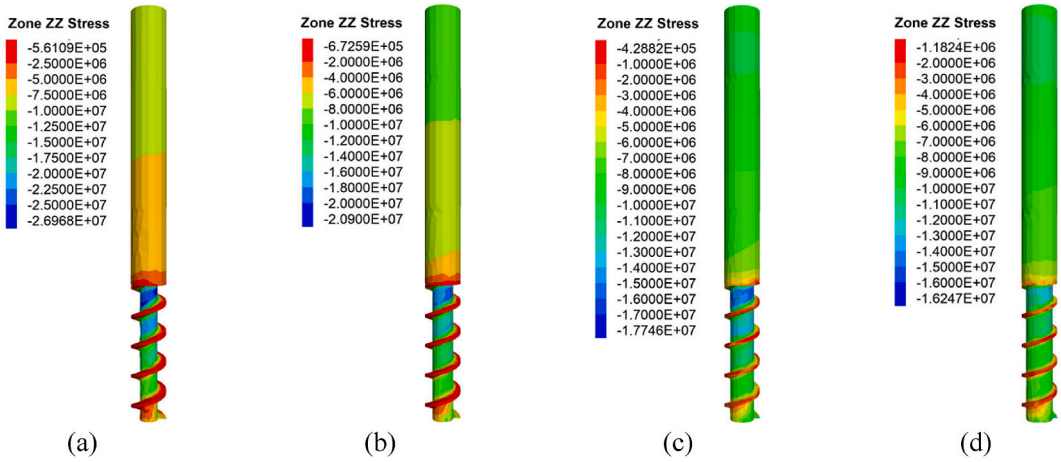

Fig. 16. Stress nephogram of the pile (a: d/D = 0.5, b: d/D = 0.58, c: d/D = 0.67, d: d/D = 0.75).

that increasing the root diameter reduced the stress concentration. This reduction in stress concentration is attributed to the increased compressive stiffness (*EA*) resulting from larger root diameters. Screw-shaft piles with root diameters of 350 mm (d/D = 0.58) or 400 mm (d/D = 0.67) exhibited superior side resistance, higher load-bearing capacity, and reduced stress concentration in the variable section area. Based on these findings, it can be concluded that a root diameter within the range of 0.58D to 0.67D is recommended

suitable for optimal performance.

4.5. Modulus of cushion

The proper installation of a cushion plays a crucial role in distinguishing between composite and pile foundations. The cushion facilitates stress distribution between the pile and ground, enabling load sharing between these elements, as reported in the literature [24]. Variations in the cushion modulus led to differences in the depth to which the pile tip penetrated the cushion, thereby influencing the stress distribution within the piles and surrounding soil. In this study, cushion moduli of 20, 40, 60, and 80 MPa were selected for computational analysis.

Fig. 17 illustrates the load-settlement characteristics of composite foundations consisting of screw-shaft piles with varying cushion moduli, showing substantial settlement within the reinforced region for a cushion elastic modulus of 20 MPa. As the cushion modulus increases, the settlement in the reinforced area gradually decreases. However, further increases in the cushion modulus did not reduce the settlement of the composite foundations proportionally. This suggests that excessively high cushion moduli have limited effectiveness in significantly reducing composite foundation settlement.

Fig. 18 shows the distribution curves of the pile-soil stress ratio for the composite foundations of screw-shaft piles with different cushion moduli. As the cushion modulus increased, the stress ratio between the pile and ground steadily increased, indicating that the pile bore a larger proportion of the load under the same applied force. Under favorable soil properties, a higher cushion modulus may not fully utilize the bearing capacity of the soil, potentially leading to economic inefficiency and wastage.

5. Conclusions

This study presents a comprehensive evaluation of the performance of composite pile foundations with screw-shaft piles by employing both laboratory model tests and numerical simulations. The investigation of various geometrical parameters of the screw-shaft piles and cushion modulus revealed the following key findings.

1. Composite foundations incorporating screw-shaft piles demonstrate a remarkable increase in load-carrying capacity of approximately 82 % compared to those with straight piles.
2. To minimize settlement in monopile composite foundations, it is advantageous to increase the proportion of threaded sections in the screw-shaft piles. The recommended range for the proportion of threaded sections is between 44 % and 55 %.
3. An approximate thread pitch of 1D is considered optimal for achieving the desired mechanical bite and enhancing side resistance; however, it is important to avoid thread pitches that are either too tight or too loose.
4. A root diameter within the range of 0.58D to 0.67D is suggested as reasonable because it improves the mechanical bite between the pile and soil without causing undue stress concentration effects.
5. The appropriate cushion modulus range of 40 MPa–60 MPa was determined based on an analysis of the P–S curves and pile-to-soil stress ratio, which affects the pile-to-soil ratio and settlement of composite foundations.

The screw-shaft pile composite foundation has been successfully utilized in practical projects, such as the foundation treatment project at Sanming South Station in Fujian Province, whereas the current design primarily relies on referencing other pile types without reasonable parameter selection. To address this gap, our study focused on investigating the parameters of the screw-shaft pile composite foundations and their bearing characteristics, with the aim of making this advantageous treatment method more rational and efficient. Specifically, when dealing with round gravel soil, adopting the pile geometry and bedding parameters proposed in our research can optimize the utilization of the threading advantage of screw-shaft piles. Consequently, the screw-shaft pile composite

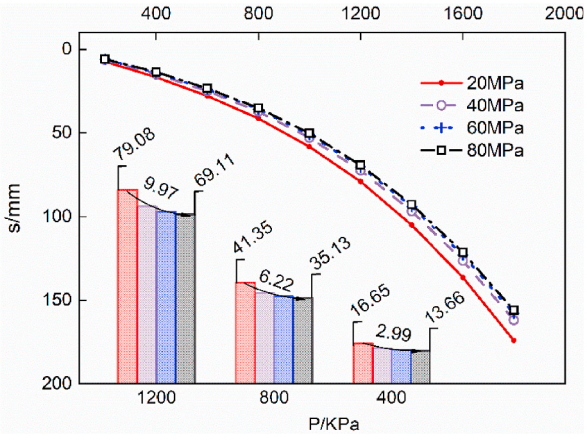

Fig. 17. Load-settlement relationships with the different modulus of the cushion.

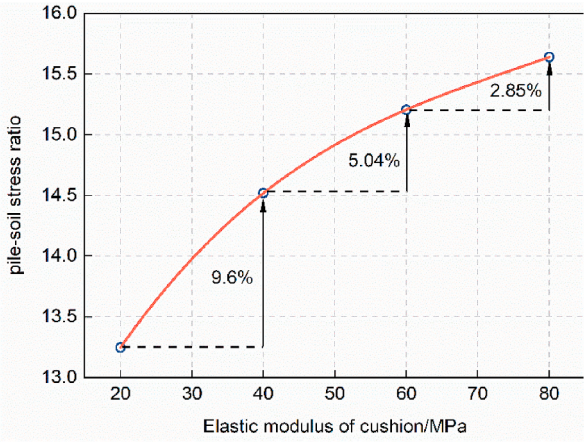

Fig. 18. The pile-soil stress ratio.

foundations can find wider applications in reinforcement treatments for railroads, highways, houses, and other structures.

Our study was limited to one type of foundation soil, whereas real-world conditions encompassed various soil types. To enhance the applicability of screw-shaft pile composite foundations, future research should analyze the load transfer mechanisms and design criteria under different soil conditions. Moreover, an essential aspect that was not considered in this study is the influence of groundwater. Future investigations should address this by analyzing the load transfer between piles and soil and comprehensively understanding the impact of groundwater on composite foundation systems, particularly in regions with high water tables and piles extending below the water table.

Funding statement

This work was supported by the Shaanxi Province Natural Science Foundation, China [grant number 2020JQ-379].The funder played no role in the study design, data collection or analysis, the decision to publish, or manuscript preparation.

Data availability statement

All data and models presented in this study are available upon request from the corresponding author.

Additional information

No additional information is available for this paper.

CRediT authorship contribution statement

Tingting Yang: Formal analysis, Methodology, Project administration, Software, Validation, Visualization, Writing – original draft. **Weicheng Zheng:** Data curation, Investigation, Supervision, Writing – original draft, Writing – review & editing. **Yongli Xie:** Conceptualization, Formal analysis, Resources. **Hongguang Zhang:** Funding acquisition, Software. **Xiabing Yue:** Resources, Supervision.

Declaration of competing interest

The authors declare that they have no known competing financial interests or personal relationships that could have appeared to influence the work reported in this paper.

Nomenclature

C_l	Length Similarity Ratio
C_A	Area Similarity Ratio
C_E	Modulus Similarity Ratio
C_F	Forces Similarity Ratio
E	Young's modulus of elasticity
ω	moisture content
C	cohesion

φ	internal friction angle
σ_i	Stress in the section "i" of the pile
ε_i	Strain in the section "i" of the pile
q_{si}	average value of side resistance in the section "i" of the pile
L_i	length of the unit in the section "i" of the pile
D	outer diameter of the pile
Q_i	average value of axial force in the section "i" of the pile
k_n	normal spring stiffness in the contact surface cell
k_s	tangential spring stiffness in the contact surface cell
K	bulk modulus
G	shear modulus
$\Delta z_{\min}$	minimum normal scale on both sides of the contact surface grid
Q_p	end resistance
Q_s	side resistance
σ_p	stress applied on the pile
σ_s	stress applied on the soil surrounding the pile
EA	Compressive stiffness

References

[1] W.T. Yang, P.P. Ni, Z. Chen, J.X. Feng, G.X. Mei, Consolidation analysis of composite ground improved by granular piles with a high replacement ratio considering overlapping smear zones, Comput. Geotech. 162 (2023), 105636, https://doi.org/10.1016/j.compgeo.2023.105636.

[2] H.M. Ma, C. Peng, Analysis and application of ultimate bearing capacity of squeezed branch pile, Geotech. Geol. Eng. 41 (6) (2023) 3823–3828, https://doi.org/10.1007/s10706-023-02461-1.

[3] L. Xiong, G.W. Li, Y. Zhou, G.J. He, Experimental and analytical investigation of the bearing capacity of bulbs for squeezed branch piles, Int. J. GeoMech. 23 (5) (2023), 04023045, https://doi.org/10.1061/IJGNAI.GMENG-8298.

[4] T. Honda, Y. Hirai, E. Sato, Uplift capacity of belled and multi-belled piles in dense sand, soils, Found 51 (3) (2011) 483–496, https://doi.org/10.3208/sandf.51.483.

[5] S.N. Moghaddas Tafreshi, S. Javadi, A.R. Dawson, Influence of geocell reinforcement on uplift response of belled piles, Acta Geotechnica: An International journal for Geoengineering. 9 (3) (2014) 513–528, https://doi.org/10.1007/s11440-013-0300-1.

[6] K. Ilamparuthi, E.A. Dickin, The influence of soil reinforcement on the uplift behaviour of belled piles embedded in sand, Geotext. Geomembranes 19 (1) (2001) 1–22, https://doi.org/10.1016/S0266-1144(00)00010-8.

[7] X.W. Wang, T.l. Chen, X. Wang, J.D. Li, D.R. Liu, Y.J. Zhang, D.J. Jiang, Performance of screw piles in thick collapsible loess, Case Stud. Constr. Mater. 19 (DEC) (2023), e02263, https://doi.org/10.1016/J.CSCM.2023.E02263.

[8] Y.D. Chen, A. Deng, A.T. Wang, H.S. Sun, Performance of screw-shaft pile in sand: model test and DEM simulation, Comput. Geotech. 104 (DEC) (2018) 118–130, https://doi.org/10.1016/j.compgeo.2018.08.013.

[9] S.N. Rao, Y.V.S.N. Prasad, Estimation of uplift capacity of helical anchors in clays, Journal of Geotechnical Engineering 119 (2) (1993) 352–357, https://doi.org/10.1061/(ASCE)0733-9410(1993)119:2(352).

[10] A.J. Lutenegger, Historical development of iron screw-pile foundations: 1836–1900, Int. J. Hist. Eng. Technol. 81 (1) (2011) 108–128, https://doi.org/10.1179/175812109X12547332391989.

[11] Y.S. Ye, D.G. Cai, X.B. Chen, Y.L. Yang, F. Chen, In-situ test study on lateral friction of screw pile composite foundation of high speed railway, China Railw. Sci. 41 (2) (2020) 1–10, https://doi.org/10.3969/j.issn.1001-4632.2020.02.01.

[12] X.Y. Cheng, Research on soft soil foundation reinforcement technology of high-speed railway beam yard based on screw pile, Railw. Constr. Tech. (1) (2022) 139–142, https://doi.org/10.3969/j.issn.1009-4539.2022.01.030.

[13] S.L. Jin, Research on bearing mechanism and applicability of shaft-screw pile group pile foundation in building structure, Build. Struc. 51 (18) (2021) 143–148, https://doi.org/10.19701/j.jzjg.2021.18.022.

[14] C. Srijaroen, M. Hoy, S. Horpibulsuk, R. Rachan, A. Arulrajah, Soil–cement screw pile: alternative pile for low- and medium-rise buildings in soft bangkok clay, J. Constr. Eng. M. 147 (2) (2021), 04020173, https://doi.org/10.1061/(asce)co.1943-7862.0001988.

[15] A. Perko Howard, Helical Piles:A Practical Guide to Design and Installation, John Wiley & Sons, Inc., New Jersey, 2009.

[16] A.A. Malik, J. Kuwano, S. Tachibana, T. Maejima, End bearing capacity comparison of screw pile with straight pipe pile under similar ground conditions, Acta Geotechnica 12 (2) (2017) 415–428, https://doi.org/10.1007/s11440-016-0482-4.

[17] Z. Meng, J.J. Chen, J.H. Wang, Numerical analysis of bearing capacity of drilled displacement piles with a screw-shaped shaft in sand, Mar. Georesour. Geotec. 35 (5) (2017) 661–669, https://doi.org/10.1080/1064119x.2016.1213777.

[18] B.h. Shen, Lecture on new technology of pile foundation construction (IX) screw pile and screw-shaft pile, Construction Machinery & Maintenance (1) (2011) 136+138–141, https://doi.org/10.3969/j.issn.1006-2114.2011.01.029.

[19] P.C. Jiang, Y.J. Zhang, W. Xu, Analysis of the bearing behaviour of a screw-pile foundation in silt soil, Proc. Inst. Civ. Eng-Gr. 172 (4) (2019) 257–263, https://doi.org/10.1680/jgrim.18.00055.

[20] L. Xu, Study on the Test and the Load-Bearing Characteristics of Half-Screw Pile, Master Thesis, Hefei Polytechnic University, Hefei, 2013.

[21] Y.D. Chen, A. Deng, F. Lu, H.S. Sun, Failure mechanism and bearing capacity of vertically loaded pile with partially-screwed shaft: experiment and simulations, Comput. Geotech. 118 (FEB) (2020), 103337, https://doi.org/10.1016/j.compgeo.2019.103337.

[22] W. Guan, H.G. Wu, S.J. Yu, S.G. Wu, Z.R. Zhu, Experimental study on dynamic and bearing characteristics of part-screw pile composite foundations under train loads, Chin. J. Rock Mech. Eng. 42 (2) (2023) 508–520, https://doi.org/10.13722/j.cnki.jrme.2022.0475.

[23] S.G. Wang, Z. Feng, J.Z. Tang, Z.P. Zhao, Experimental study on bearing mechanism of screw cast-in-place piles under vertical loads, Chin, J. Geotech. Eng. 43 (2) (2021) 383–389, https://doi.org/10.11779/CJGE202102019.

[24] P.C. Jiang, Comparative analysis on bearing behaviors of CFG pile and screw pile composite foundation in silt foundation, J. Chin. Railw. Soc. 41 (4) (2019) 125–132, https://doi.org/10.3969/j.issn.1001-8360.2019.04.017.

[25] M. Sakr, Performance of helical piles in oil sand, Can. Geotech. J. 46 (9) (2009) 1046–1061, https://doi.org/10.1139/t09-044.

[26] G. Spagnoli, C.D.H. Cavalcanti Tsuha, A review on the behavior of helical piles as a potential offshore foundation system, Mar. Georesour. Geotec. 38 (9) (2020) 1013–1036, https://doi.org/10.1080/1064119X.2020.1729905.

[27] A. Mohajerani, D. Bosnjak, D. Bromwich, Analysis and design methods of screw piles: a review, Soils Found. 56 (1) (2016) 115–128, https://doi.org/10.1016/j.sandf.2016.01.009.

[28] M. Sakr, Installation and performance characteristics of high capacity helical piles in cohesionless soils, DFI J. J. Deep Found. 5 (1) (2011) 39–57, https://doi.org/10.1179/dfi.2011.004.

[29] G.G. Meyerhof, A study of anchorages for transmission tower foundations: discussion, Can. Geotech. J. 9 (3) (1972) 321–322, https://doi.org/10.1139/t72-036.

[30] S.A. Stanier, J.A. Black, C.C. Hird, Modelling helical screw piles in soft clay and design implications, P. I. Civil. Eng-Geotec. 167 (5) (2014) 447–460, https://doi.org/10.1680/geng.13.00021.

[31] K. Shao, Q. Su, J.W. Liu, K.W. Liu, Z.P. Xiong, T.F. Wang, Optimization of inter-helix spacing for helical piles in sand, J. Rock. Mech. Geotech. 14 (3) (2022) 936–952, https://doi.org/10.1016/j.jrmge.2021.11.007.

[32] H.W. Ma, L. Liu, P. Wang, S. Yuan, Q.R. He, X.L. Yang, Calculation method and mechanism of ultimate side resistance of screw pile, Mar. Georesour. Geotec. 41 (1) (2021) 99–113, https://doi.org/10.1080/1064119X.2021.2014003.

[33] F. Fatnanta, S. Satibi, Muhardi, Bearing capacity of helical pile foundation in peat soil from different, diameter and spacing of helical plates, in: Quality in Research: International Symposium on Materials, Metallurgy, and Chemical Engineering, vol. 316, 2018, 012035, https://doi.org/10.1088/1757-899X/316/1/012035.

[34] B.E. George, S. Banerjee, S.R. Gandhi, Numerical analysis of helical piles in cohesionless soil, Int. J. Geotech. Eng. 14 (4) (2020) 361–375, https://doi.org/10.1080/19386362.2017.1419912.

[35] A.S. Jamill, H.O. Abbas, Effect of screw piles spacing on group compressive capacity in soft clay, in: 2nd International Scientific Conference of Engineering Sciences, vol. 1076, 2021, 012098, https://doi.org/10.1088/1757-899X/1076/1/012098.

[36] H.O. Abbas, O.K. Ali, Parameters affecting screw pile capacity embedded in soft clay overlaying dense sandy soil, in: The Fourth Scientific Conference for Engineering and Postgraduate Research, vol. 745, 2020, 012117, https://doi.org/10.1088/1757-899X/745/1/012117.

[37] M.A. Saleem, A.A. Malik, J. Kuwano, Model study of screw pile installation impact on ground disturbance and vertical bearing behaviour in dense sand, in: 18th Nordic Geotechnical Meeting, vol. 710, 2021, 012056, https://doi.org/10.1088/1755-1315/710/1/012056.

[38] F. Bagheri, M.H. El Naggar, Effects of installation disturbance on behavior of multi-helix piles in structured clays, DFI J. J. Deep Found. 9 (2) (2015) 80–91, https://doi.org/10.1179/1937525515y.0000000008.

[39] B. Livneh, M.H. El Naggar, Axial testing and numerical modeling of square shaft helical piles under compressive and tensile loading, Can. Geotech. J. 45 (8) (2008) 1142–1155, https://doi.org/10.1139/t08-044.

[40] C.W. Li, J.J. Chen, Q. Wu, X.H. Xia, J.H. Wang, Bearing mechanism and calculation method of screw pile, Journal of Shanghai Jiaotong University 44 (6) (2010) 726–730, https://doi.org/10.16183/j.cnki.jsjtu.2010.06.002.

[41] V. Vignesh, M. Mayakrishnan, Design parameters and behavior of helical piles in cohesive soils-A review, Arab. J. Geosci. 13 (22) (2020) 1194, https://doi.org/10.1007/s12517-020-06165-1.

[42] M. Aydin, T.D. Bradka, D.A. Kort, Osterberg cell load testing on helical piles, in: Geo-frontiers Congress 2011, 2011, pp. 66–74, https://doi.org/10.1061/41165(397)8.

[43] M.H. El Naggar, M.A. Youssef, M. Ahmed, Monotonic and cyclic lateral behaviour of helical pile specialized connectors, Eng. Struct. 29 (10) (2007) 2635–2640, https://doi.org/10.1016/j.engstruct.2007.01.018.

[44] Z. Meng, J.J. Chen, L.Y. Zhang, J.H. Wang, J.M. Yao, Field tests to investigate the installation effects of drilled displacement piles with screw-shaped shaft in clay, J. Geotech. Geoenviron. 141 (12) (2015), 06015010, https://doi.org/10.1061/(ASCE)GT.1943-5606.0001371.

[45] J.Z. Hu, Bearing Capacity Behavior of Roll Forming Screw Pile, Master Thesis, Beijing Jiaotong University, Beijing, 2008.

[46] W.M. Leng, G.S. Wei, R.S. Nei, L.M. Wei, J.L. Dong, Research on the vertical bearing characteristics and bearing mechanism of screw pile, J. Railw. Eng. Soc. 37 (5) (2020) 1–6+35, https://doi.org/10.3969/j.issn.1006-2106.2020.05.001.

[47] C.H. Xu, X.D. Zhang, X.Y. Xu, Application study on design parameters of cast-in-place concrete screw pile, Ind. Constr. 40 (10) (2010) 91–94, https://doi.org/10.13204/j.gyjz2010.10.019.

[48] J.J. Zheng, S.W. Abusharar, X.Z. Wang, Three-dimensional nonlinear finite element modeling of composite foundation formed by CFG–lime piles, Comput. Geotech. 35 (4) (2007) 637–643, https://doi.org/10.1016/j.compgeo.2007.10.002.

[49] Y.P. Shen, H.H. Wang, Optimization design on CFG-pile foundation with different cushion thickness in beijing-shanghai high-speed railway, Transportation Infrastructure Geotechnology 3 (1) (2016) 3–20, https://doi.org/10.1007/s40515-015-0026-7.

[50] P. Halder, B. Manna, Large scale model testing to investigate the influence of granular cushion layer on the performance of disconnected piled raft system, Acta Geotechnica 16 (5) (2021) 1–18, https://doi.org/10.1007/S11440-020-01121-5.

[51] A. Ata, E. Badrawi, M. Nabil, Numerical analysis of unconnected piled raft with cushion, Ain Shams Eng. J. 2 (2) (2014) 1–8, https://doi.org/10.1016/j.asej.2014.11.002.

[52] H.G. Harris, G.M. Sabnis, Structural Modeling and Experimental Techniques, CRC Press, Boca Raton, 1999.

[53] M. Bolton, M.W. Gui, J.P. Garnier, J. Corté, G. Bagge, J. Laue, R. Renzi, Centrifuge cone penetration tests in sand, Geotechnique 49 (4) (1999) 543–552, https://doi.org/10.1680/geot.1999.49.4.543.

[54] Ministry of Housing and Urban Rural Construction of the People's Republic of China, *Code for Design of Concrete Structures*. GB 50010-2010, MOHURD, Beijing, China, 2010.

[55] Ministry of Housing and Urban Rural Construction of the People's Republic of China, *Technical Code for Ground Treatment of Buildings*. JGJ 79-2012, MOHURD, Beijing, China, 2012.

[56] N.K. Ovesen, The scaling law relationship: panel discussion, in: 7th European Conference on Soil Mechanics and Foundation Engineering, vol. 4, 1979, pp. 319–323.

[57] H.B. Xiao, Q.Z. Luo, J. Tang, Q.S. Li, Prediction of load–settlement relationship for large-diameter piles, Struct. Des. Tall Special Build. 11 (4) (2010) 285–293, https://doi.org/10.1002/tal.201.

[58] M.H. Zhao, H.Y. Niu, M. Liu, X. Tan, Pile-soil stress ratio and settlement of composite ground with gravel piles in flexible foundation, Chin. J. Geotech. Eng. 39 (9) (2017) 1549–1556, https://doi.org/10.11779/CJGE201709001.

[59] H.Y. Zhang, H.L. Ma, Experimental study on the effect of pile-end soil on the pile load transfer law, Appl. Sci. 12 (13) (2022) 6347, https://doi.org/10.3390/app12136347.